Proc. Camb. Phil. Soc. (1973), **74**, 217
PCPS 74–2
With 8 *text-figures*
Printed in Great Britain

Zeeman's Catastrophe Machine

By T. POSTON and A. E. R. WOODCOCK
Mathematical Institute, The University of Warwick

(*Received* 24 *June* 1972)

René Thom (5) has shown that if the state of a system is determined by the local minimization of a potential – that is, if the system is so highly dissipative that transients can safely be ignored – then, though a smooth change in the potential function may give rise to a discontinuous change of state, the ways in which this can happen are quite limited. In fact, if we have at most a four-parameter family of potentials, discontinuities of this kind can occur in only seven ways up to local diffeotype, if they are to be structurally stable. (This latter condition is the requirement that it be impossible to alter the discontinuity type by an arbitrarily small perturbation of the family of potentials: roughly it requires that the behaviour of the system, considered as a function of possible families of potentials, be 'continuous' at the family concerned. It bears the same relationship as does continuity to computability: a computer given approximately correct data for which to compute the value of a function or the behaviour of a system will give an approximately correct answer if the function is continuous, the system structurally stable. If not, only analytic methods will serve, and the physical significance of the result will be dubious. Fortunately, in the dimensions with which we are concerned, structural stability is an open dense property in the space of possible families of potentials; thus unstable systems can be ignored for almost all purposes, just as we ignore the 'possibility' of balancing a pin on its point.)

Hence, if, for any system (physical/chemical/biological, etc.), we have grounds for assuming that it is governed through potentials by at most a four-dimensional control, we may deduce that locally any discontinuous behaviour has the form of one of Thom's seven elementary catastrophes.

In particular, with a two-dimensional control only two types of singularity are possible; the fold and the cusp. The cusp catastrophe has so far been the most fruitful of detailed applications (see in patricular Zeeman (7), (9) and Fowler (2)) and to illustrate it Zeeman (8) devised a machine using elastic energy for potentials. (Several other machines, with radically different potentials such as soap-film and gravitational energy, now exist to attest the universality of the theory). The machine is worthy of some detailed analysis, since it not only illustrates the cusp catastrophe in both its aspects but exemplifies the way in which a precise qualitative description can be both more exact and more illuminating than a precise quantitative one.

The machine consists of a wheel of radius r free to turn about the origin O, and two pieces of elastic BA, BX of unstretched length p attached to its edge. A is the fixed point $(0, -a)$, X a variable point (x, y). We consider only the open set C of those X for which the elastic is actually stretched.

https://doi.org/10.1017/S0305004100048003 Published online by Cambridge University Press

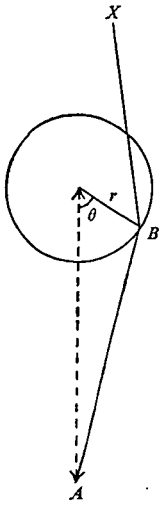


Fig. 1

Detailed suggestions for construction are given in (8).

For each X the system has energy $V_X(\theta)$ proportional to $(1-p)^2+(m-p)^2$, varying with the angle θ of the wheel. Experimentally (the reader is emphatically recommended to make and play with a machine) for some values of X the system has two stable equilibria, corresponding to local minima of V_X, and for other values only one. The curve separating these types of values of X is known as the *bifurcation set* of the system, and it is only by moving X across it that the wheel can be caused to jump rather than move smoothly with the control.

By Thom's Theorem the set

$$M = \left\{(X,\theta)\middle|\frac{dV_X}{d\theta}=0\right\} \subseteq C\times S^1$$

of equilibria (stable or otherwise) of the system is a smoothly embedded surface in the three-dimensional space $C\times S^1$, and for a suitable neighbourhood N of any singular point P of the map

$$\chi: M \to C, \quad (X,\theta) \rightsquigarrow X$$

and $\overline{N}$ of $\chi(P)$ there must be diffeomorphisms ϕ, ψ making

$$\begin{array}{ccccccc} N & \xrightarrow{\phi} & N' \subseteq M' \subseteq \mathbb{R}^3 & & (a,b,x) \\ \downarrow{\scriptstyle \chi} & & \downarrow{\scriptstyle \chi'} & & \downarrow & & \downarrow \\ \overline{N} & \xrightarrow{\psi} & \overline{N}' & \subseteq & \mathbb{R}^2 & & (a,b) \end{array}$$

commute, where either

$$M' = (a,b,x)\,x^2+a=0 \quad \text{from} \quad V_{(a,b)}(x) = \tfrac{1}{3}x^3+ax$$

or

$$M' = (a,b,x)\,x^3+ax+b=0 \quad \text{from} \quad V_{(a,b)}(x) = \tfrac{1}{4}x^4+\tfrac{1}{2}ax^2+bx,$$

respectively the equilibrium set and potential for the no. 1 catastrophe (the fold) multiplied by a trivial dimension, and the equilibrium set and potential for the no. 2

https://doi.org/10.1017/S0305004100048003 Published online by Cambridge University Press

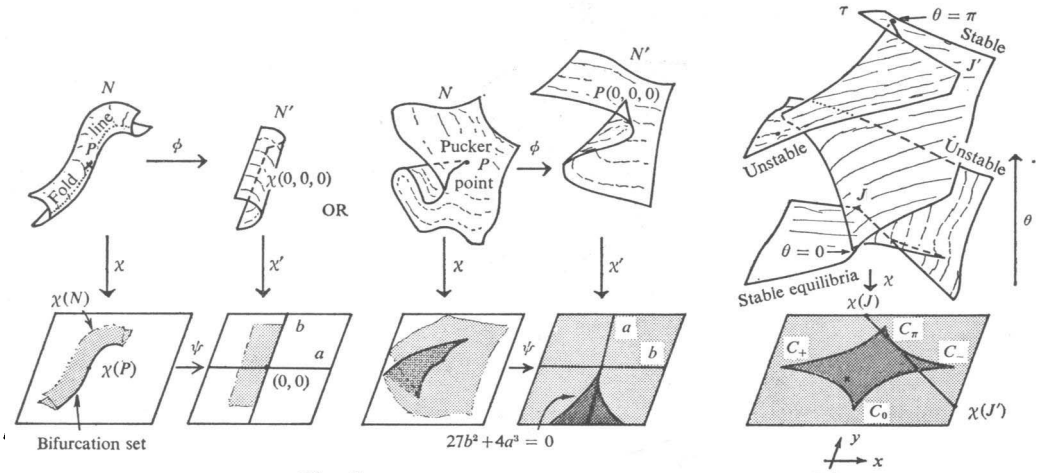


Fig. 2

Fig. 3

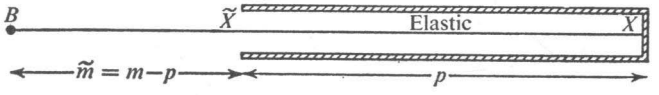


Fig. 4

catastrophe (the cusp or Riemann–Hugoniot), in their standard forms. Pictorially, the situation must hence be as in Fig. 2.

Thus the form of the bifurcation set is locally a smoothly immersed curve or a cusp (no corners are possible, for example). With this information, a little experiment, and subsidiary arguments, such as appeal to symmetry, it is easily established that the global description is as shown in Fig. 3, with the y-axis an axis of symmetry of the bifurcation set.

Only one of the two layers of surface meeting any fold line can consist of stable equilibria. Over cusp C_0 or C_π the singularity involves a layer of maxima between two of minima; there is also a layer of maxima not locally singular. Over C_+ or C_- this is reversed.

Taylor series expansion of the elastic energy in terms of θ for points on the y-axis determines the position of the vertical cusps and verifies the existence locally of ϕ and ψ (essentially, ϕ is defined by 'leaving off higher-order terms in θ' and ψ is an affine change of coordinates). Until recently, the analysis rested at that point. To proceed further, it is convenient to start with a simplifying assumption, which can be physically realized in the Mk II Catastrophe Machine.

We shall suppose that the tension in the upper piece of elastic is proportional directly to its length m, not to $(m-p)$. (To validate this physically, enclose the elastic in a tube of length p as shown in Fig. 4, and use $\tilde{X} = (\tilde{x}, \tilde{y})$ rather than X as control; varying now in $\tilde{C}$ rather than C, with the obvious definition.) Now consider the contours, i.e. lines of constant θ, in the surface M. Suppose we know that $(\tilde{x}, \tilde{y}, \theta) \in M$. That is, the wheel is in equilibrium (stable or otherwise) at θ for $\tilde{X} = (\tilde{x}, \tilde{y})$. That is, the tangential components at the point B of the tensions in the two elastics are equal (the components

https://doi.org/10.1017/S0305004100048003 Published online by Cambridge University Press

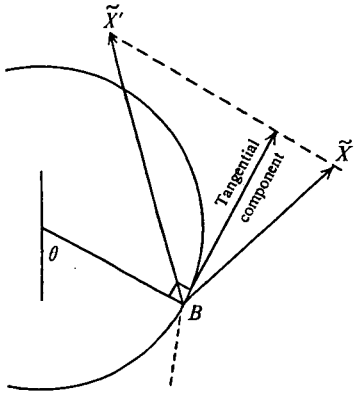


Fig. 5

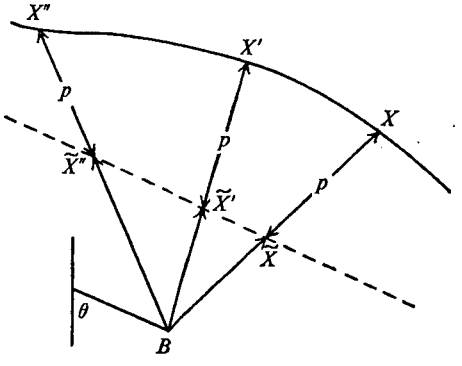


Fig. 6

radial to the wheel being killed off by the constraints). Hence, $(\tilde{X}', \theta) \in M$ also if and only if the tangential components of the tension in the upper elastic when stretched from B to $\tilde{X}$ and to $\tilde{X}'$ are equal. Now the tension $T_{\tilde{X}}$ in $B\tilde{X}$, for any $\tilde{X}$, is a vector in the direction $\mathbf{B\tilde{X}}$ and proportional to its length. Thus, with appropriate choice of scale, the force vector $T_{\tilde{X}}$ and the geometric vector $\mathbf{B\tilde{X}}$ are essentially identical. Hence $(\tilde{X}', \theta) \in M$ if and only if $\mathbf{B\tilde{X}}'$ has the same tangential component as $\mathbf{B\tilde{X}}$; that is, if and only if $\tilde{X}'$ is on the line through $\tilde{X}$ parallel to the radius of the wheel. Hence irrespective of the laws determining the 'downward' force on the wheel, the θ-contours of M are straight lines with slope $-\cot\theta$. The force law fixes only the intercept with the y-axis.

The equilibrium surface $M \leqslant \mathbb{R}^3$ of the Mk II machine is thus a ruled surface. If the projections of sufficiently many θ-contours are drawn in the (x, y)-plane (Fig. 7*a*) the bifurcation set becomes visible as their envelope – this being precisely the projection of the fold lines of M by χ.

We now return to the Mk I machine. A similar analysis applies, but now the tension is proportional not to length but to extension. Thus corresponding to a given Mk II equilibrium we have a Mk I equilibrium with the same tension $T_{\tilde{X}}$ say, hence an extension equal to the Mk II length, hence a control X in the same direction as $\tilde{X}$ from B

https://doi.org/10.1017/S0305004100048003 Published online by Cambridge University Press

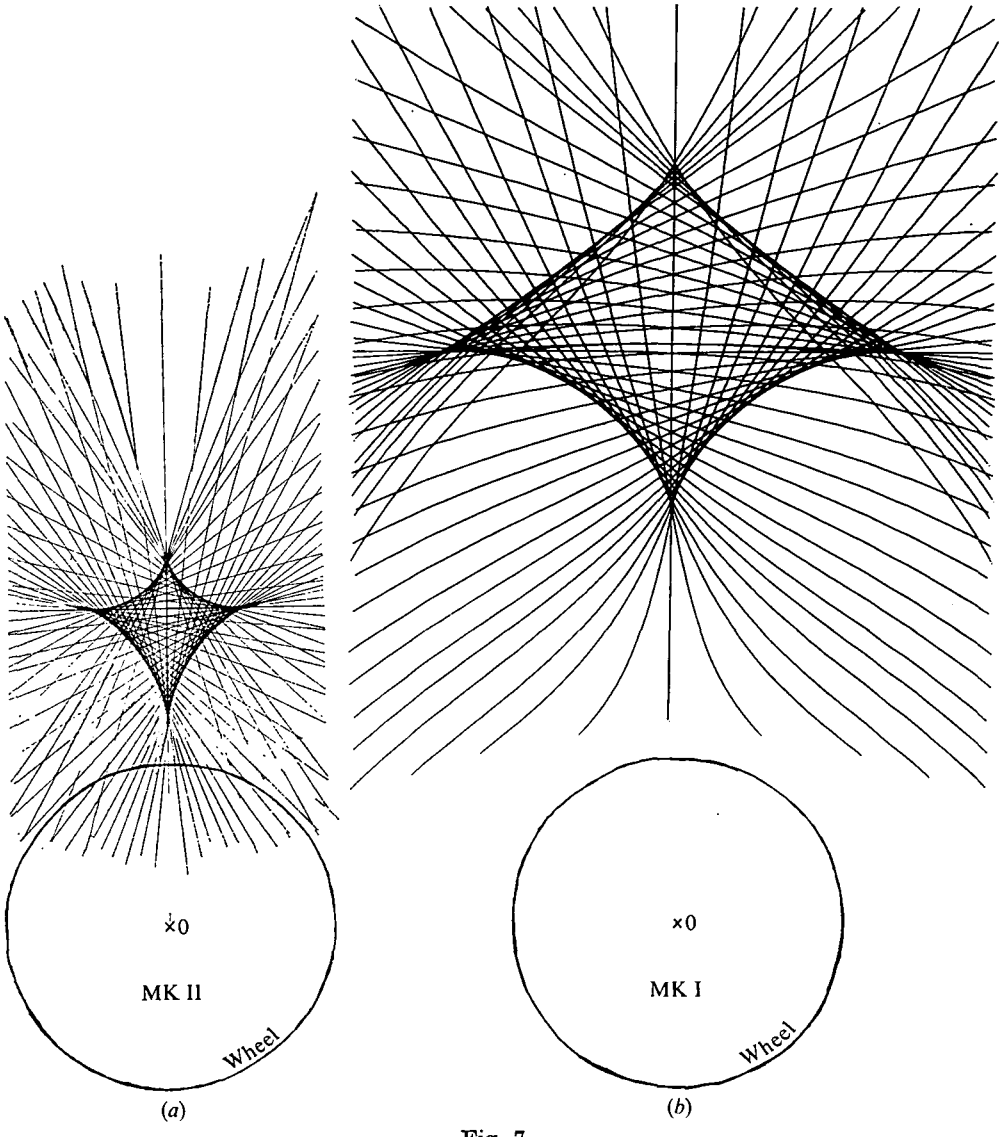


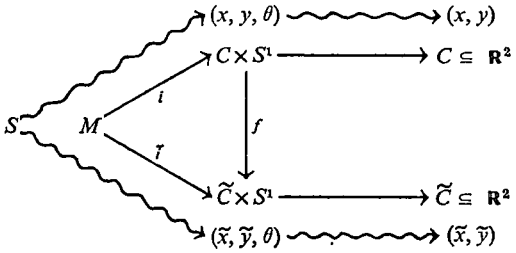
Fig. 7

but p farther away. Thus a contour will be the locus of X as $\tilde{X}$ traverses a Mk II contour. Each contour is thus a conchoid of Nichomedes (a curve invented about 150 B.C. for the purpose of trisecting angles; cf. (3), (4)). Exactly as for the Mk II machine, the envelope of these contours is the bifurcation set (Fig. 7*b*). The contours drawn in Fig. 7 (*b*) are the conchoids corresponding to the straight lines of Fig. 7 (*a*), and the values of a, p and r are the same for same for the two figures.

This method of drawing the bifurcation set indirectly by means of the contours is not only simpler but more illuminating than drawing it directly, since it displays the way in which M is projected. It is universally appropriate; both in detailed applications, as here, and in drawing the standard forms of the catastrophes (6).

https://doi.org/10.1017/S0305004100048003 Published online by Cambridge University Press

The positions of the cusps in the two machines are not simply related. Since every Mk I machine contains a Mk II machine (by the purely labelling device of the tube) and vice versa, we may think of the surface M of equilibrium states as embedded in two ways in $\mathbb{R}^2 \times S^1$; a state S can be represented either as (x, y, θ) or as $(\tilde{x}, \tilde{y}, \theta)$, and we have a commutative diagram



where f is the level-preserving diffeomorphism

$$(x, y, \theta) \rightsquigarrow \left(x - \frac{p(x - r\sin\theta)}{(x^2+y^2+r^2-2rx\sin\theta+2ry\cos\theta)^{\frac{1}{2}}},\ y - \frac{p(y+r\cos\theta)}{(x^2+y^2+r^2-2rx\sin\theta+2ry\cos\theta)^{\frac{1}{2}}},\ \theta\right)$$

and we have $\chi = \pi i$, $\tilde{\chi} = \tilde{\pi}\tilde{\imath}$.

No map $C \to \tilde{C}$ will make the diagram commute: the surface is 'rolled round' by f between the two projections, so that the fold lines and pucker points occur at different places on it. This emphasizes that the singularities are in the projection, *not* in the catastrophe surface itself, which is, in general, smooth and in the standard case analytic.

By techniques of an older generation (no longer taught in most places – particularly not in those which go in for courses in topics like catastrophe theory, for which they are a necessity: in this particular case retrieved from (1)) we find that the explicit equation for the envelope bifurcation set of the Mk II machine, parametrized by the angle θ of the wheel, is

$$(x, y) = \left(-\frac{a^2 pr\sin^3\theta}{(a^2+r^2-2ar\cos\theta)^{\frac{3}{2}}},\ a - \frac{ap(a^2+r^2+3ar\cos\theta-ar\cos^3\theta)}{(a^2+r^2-2ar\cos\theta)^{\frac{3}{2}}}\right).$$

Notice that if we fix a, the possible figures are all similar: for $p = a - r$ (i.e. for the lower elastic just taut when $\theta = 0$, so this is the greatest value of p we can use unless we substitute a spring), the lower cusp is at the centre of the wheel, and shortening the elastic contracts the whole figure – both contours and bifurcation set – towards the point $(0, a)$ exactly opposite the fixed point of the lower elastic, proportionately to p. Fig. 8 illustrates this for $a = 4$, $r = 1$, $p = 3, 2\frac{3}{4}, \ldots, \frac{1}{2}$. By geometrical arguments extending those that showed the contours to be straight, altering the relaxed length of the upper elastic on its own simply dilates or contracts the figure from or towards $(0, 0)$. Thus the similarity type of the figure is fixed by the ratio r/a; altering the other quantities such as the lengths of the elastic merely changes its size and position.

https://doi.org/10.1017/S0305004100048003 Published online by Cambridge University Press

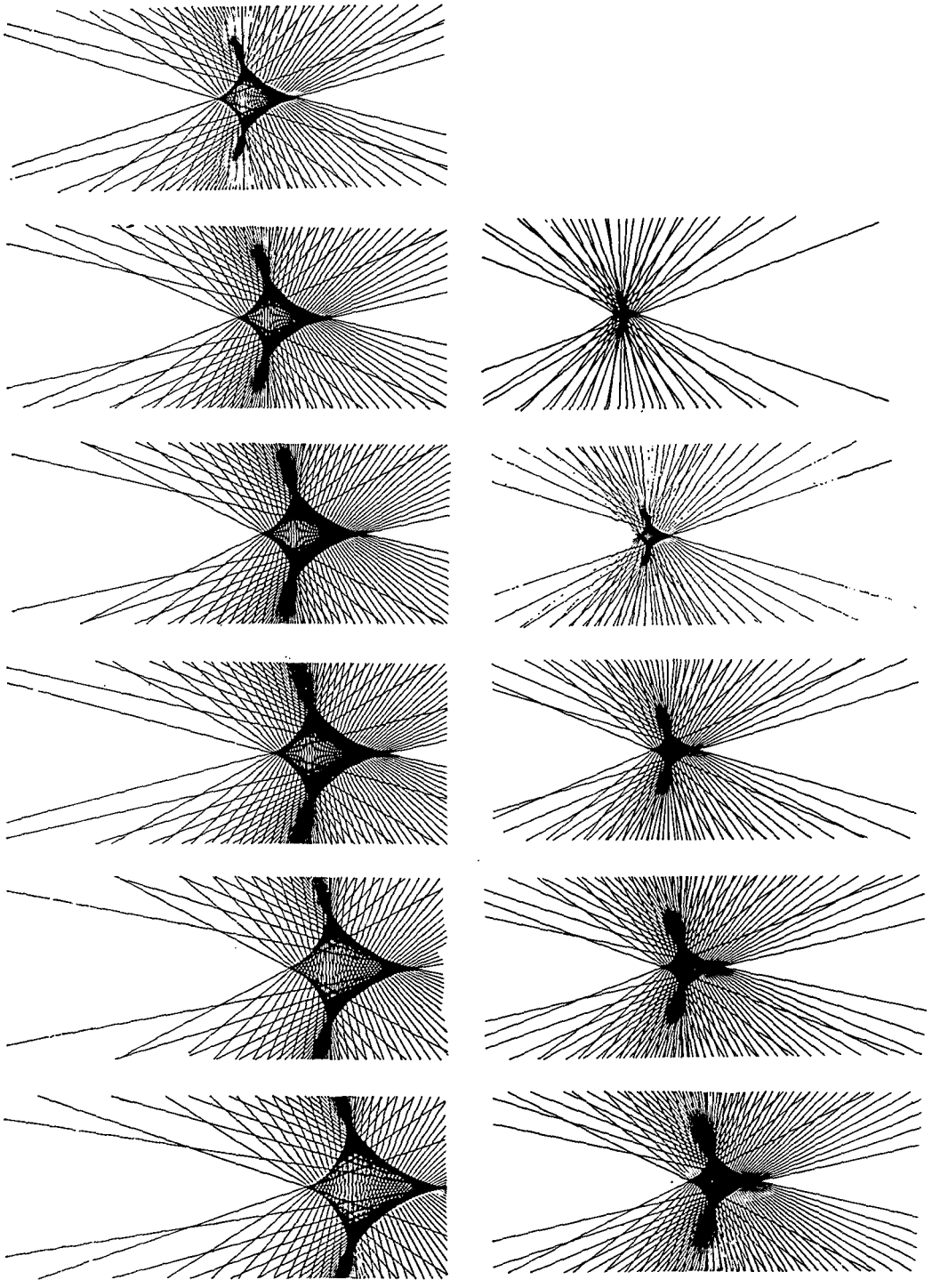


Fig. 8

https://doi.org/10.1017/S0305004100048003 Published online by Cambridge University Press

By further differentiation we find that the vertical cusps are at the points,

$$O, \quad \frac{a(a \pm r - p)}{(a \pm r)},$$

and the side cusps at

$$\pm \frac{pr}{a}, \quad a - \frac{p(a^2+r^2)}{a^3\sqrt{(a^2-r^2)}}.$$

The side cusps point upwards at an angle of $\cos^{-1}(r/a)$ to the vertical, and hence correspond to states where the lower elastic is tangential to the wheel, on the other side of the y-axis. The referee has pointed out that this may also be shown geometrically, as follows:

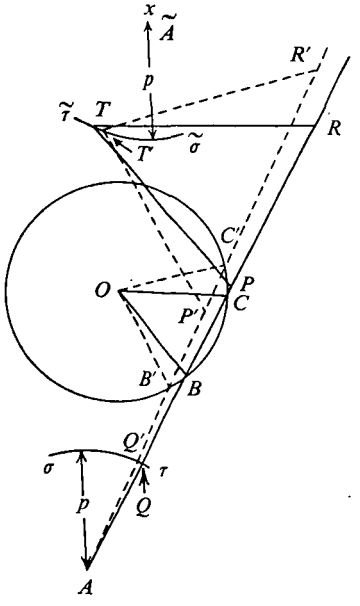


Fig. 9

Each secant of the wheel from A corresponds to two values of θ. On each such secant mark Q such that $AQ = p$, and P, R such that $BP = BQ$, $CR = CQ$. Then the wheel is in equilibrium at B with the control at P, at C with the control at R, since the forces in the upper and lower elastics are then equal and opposite. Hence the contours for these positions of the wheel are the lines PT, RT parallel to BO, CO, intersecting at T.

Now, for any such secant, T is the reflexion in O of Q, by a simple argument using similar triangles. Therefore as Q varies over the arc $\sigma\tau$ centred on A, T varies over the arc $\tilde{\sigma}\tilde{\tau}$ centred on $\tilde{A} = (0, a)$, the reflexion of A in O. Moreover, if we consider a nearby secant $A'B'C'$, we have the intersections of PT with $P'T'$, RT with $R'T'$ inside the segments PT, RT; hence so are the characteristic points, where PT, RT touch the envelope. These must coincide at $\tilde{\tau}$ for $Q = \tau$, at $\tilde{\sigma}$ for $Q = \sigma$, and must approach $\tilde{\sigma}$ and $\tilde{\tau}$ tangentially to the outward directions of $\tilde{\sigma}\tilde{\tau}$; the side cusps thus lie at $\tilde{\sigma}$ and $\tilde{\tau}$.

This also accounts geometrically for the behaviour illustrated in Fig. 8; as p is decreased, the arc $\sigma\tau$ is contracted towards A and hence the arc $\tilde{\sigma}\tilde{\tau}$ towards $\tilde{A}$,

https://doi.org/10.1017/S0305004100048003 Published online by Cambridge University Press

carrying the side cusps along with it. The similarity of the figures follows from the observation that the directions of the contours through any point T on $\tilde{\sigma}\tilde{\tau}$ depend only on the angle $\angle O\tilde{A}T$, not on the length p.

The Mk I machine is a little more complicated. The bifurcation set, again parametrized by θ, is given implicitly by the (x, y) solutions of the equations

$$O = a\sin\theta - \frac{ap\sin\theta}{(a^2+r^2-2ar\cos\theta)^{\frac{1}{2}}} - (y\sin\theta + x\cos\theta)\left(1 - \frac{p}{(x^2+y^2+r^2-2rx\sin\theta+2ry\cos\theta)^{\frac{1}{2}}}\right),$$

$$O = (y-a)\cos\theta - x\sin\theta + ap\left(\frac{(a^2+r^2)\cos\theta - ar(3\cos^2\theta-1)}{(a^2+r^2-2ar\cos\theta)^{\frac{3}{2}}}\right) + p\left(\frac{\begin{array}{r}x^3\sin\theta - y^3\cos\theta - xy(x\cos\theta - y\sin\theta - 3r\sin\theta\cos\theta) - rx^2(\sin^2\theta+1) \\ - ry^2(\cos^2\theta+1) + r^2(x\sin\theta - y\cos\theta)\end{array}}{(x^2+y^2+r^2-2rx\sin\theta+2ry\cos\theta)^{\frac{3}{2}}}\right).$$

From these equations, the vertical cusps are found to lie at

$$O, \quad \frac{(a\pm r)^2 \pm pr + \sqrt{[pr(8ar \pm 6a^2 + pr \pm 2r^2) + (a^2+r^2)^2]}}{2(a\pm r)}$$

with '$-$' chosen from '$\pm$' for the lower cusp, '$\mp$' for the upper cusp. For $r = \frac{1}{2}, p = 1$ and $a = 2$, the values for which Fig. 7 was drawn, this gives cusps at

$$O, \quad \frac{7+\sqrt{97}}{12} \quad \text{and} \quad O, \quad \frac{27+\sqrt{489}}{20}$$

in agreement with the picture as drawn, the result of the power series approach referred to above, and experiment.

The reader may care to amuse himself by finding a precise formula for the positions of the side cusps in this case. Mathematically, they are the points satisfying the pair of equations above and also

$$\frac{dx}{d\theta} = 0 = \frac{dy}{d\theta}, \quad \sin\theta \neq 0.$$

(It is clear from the picture that $dx/d\theta = 0$; $\sin\theta \neq 0$ will suffice to determine the positions completely.)

REFERENCES

(1) Edwards, J. *An elementary treatise on the differential calculus, with applications and numerous examples* (Macmillan, London, 1892).

(2) Fowler, D. The Riemann–Hugoniot catastrophe and Van der Waal's equation. In *Towards a theoretical biology*, vol. iv, ed. C. H. Waddington (Edinburgh University Press, to appear.)

(3) Klein, F. *Famous problems of elementary geometry* (Göttingen 1895, 1897, trans. Wooster Woodruff Beman & David Eugene Smith, most recent edition Chelsea Publishing Co., New York, 1962).

(4) Pappus of Alexandria, Bk iv, Synagoge, *circa* A.D. 300.

https://doi.org/10.1017/S0305004100048003 Published online by Cambridge University Press

(5) THOM, R. *Stabilité structurelle et morphogénèse* (to appear).
(6) WOODCOCK, A. E. R. and POSTON, T. *The geometry of the elementary catastrophes* Springer-Verlag, Lecture Notes in Mathematics, to appear).
(7) ZEEMAN, E. C. Differential equations of the heartbeat and nervous impulse. In *Towards a theoretical biology*, vol. IV, ed. C. H. Waddington (Edinburgh University Press, to appear).
(8) ZEEMAN, E. C. A catastrophe machine. In *Towards a theoretical biology*, vol. IV, ed. C. H. Waddington (Edinburgh University Press, to appear).
(9) ZEEMAN, E. C. Applications of catastrophe theory. *Bull. Lond. Math. Soc.* (to appear).

https://doi.org/10.1017/S0305004100048003 Published online by Cambridge University Press